

TENSILE PROPERTIES AND MICROSTRUCTURAL CHARACTERIZATION OF HI-NICALON SiC/RBSN COMPOSITES

Ramakrishna.T. Bhatt

NASA Lewis Research Center
21000 Brookpark Road
Cleveland, OH, 44135

The room temperature physical and mechanical properties of silicon carbide fiber-reinforced reaction-bonded silicon nitride matrix composites (SiC/RBSN) were measured, and the composite microstructure was analyzed. The composites consist of nearly 24 vol% of aligned Hi-Nicalon SiC fiber yarns in a ~30 vol% porous silicon nitride matrix. The fiber yarns were coated by chemical vapor deposition with a 0.8 μ m layer of boron nitride (BN) followed by a 0.2 μ m layer of SiC. In the as-fabricated condition, both 1-D and 2-D composites exhibited high strength and graceful failure, and showed improved properties when compared with unreinforced matrix of comparable density. No indication of reaction between the SiC fiber and BN coating was noticed, but the outer SiC layer reacted locally with the nitridation enhancing additive in the RBSN matrix. A comparison is made between the predicted and measured values of matrix cracking strength.

1. INTRODUCTION

Reaction-bonded silicon nitride (RBSN) has long been considered a candidate material for hot section structural components in advanced heat engine applications^{1,2}. The main attributes of RBSN are ease of fabrication, near net shape capability, high creep resistance, high-temperature strength, and low density. In spite of these advantages, RBSN is not used for commercial applications because of

its low fracture strength and fracture toughness at room temperature, and high internal oxidation rates between 800 and 1000°C. Although its strength properties can be improved by controlling the processing variables or by post-fabrication treatments³, and its internal oxidation problems can be alleviated by chemically vapor depositing a dense layer of Si_3N_4 or by infiltrating the porous body with a Si_3N_4 -yielding polymer^{4,5}, its fracture toughness cannot be altered to any perceptible degree by conventional processing methods. A solution to this problem is to reinforce the RBSN with high modulus, high strength ceramic fibers. Previous studies have shown that strong and tough SiC/RBSN composites can be fabricated by reinforcing RBSN with 144- μm -diameter SiC fibers⁶. Although this composite has been used as a model system to study structure and property correlation, it cannot be used for high-temperature applications for two reasons: (1) it has limited shape capability because the large diameter fibers cannot be bent to a radius less than 12 mm and (2) it is prohibitively expensive to machine complex-shaped components from a composite block. Both of these problems can be overcome by choosing small diameter ($\approx 14 \mu\text{m}$) SiC fibers as reinforcement.

Polymer derived small diameter SiC fibers such as CG Nicalon and Tyranno fibers that were coated with a thin layer ($\sim 1 \mu\text{m}$) of carbon or BN have been explored earlier as reinforcement for RBSN⁷⁻⁹. Although in most cases limited strain capability beyond matrix fracture was demonstrated, the ultimate fracture strength was low because of strength degradation of the fibers during high temperature nitridation. In recent years second generation small diameter SiC fibers such as Hi-Nicalon, Hi-Nicalon-S, and Sylramic fibers with better thermal stability than the first generation SiC fibers have been developed^{10, 11}. In a recent investigation, Bhatt and Hull¹² studied strength properties of coated Hi-Nicalon SiC fiber/RBSN tow composites processed under RBSN processing conditions.

Fiber coatings were either pyrolytic boron nitride (PBN), PBN/Si-rich PBN, or boron nitride (BN)/SiC. This study concluded that all three CVD coated Hi-Nicalon SiC fibers are stable through the RBSN processing condition, but BN/SiC coated tow composites yielded greater strength retention than the other two tow composites.

The objectives of this study were to fabricate BN/SiC coated Hi-Nicalon SiC/RBSN composites, and to evaluate its room temperature mechanical properties and characterize its microstructure.

2. EXPERIMENTAL

2.1. Materials

The SiC fiber yarn (Hi-Nicalon) required for composite fabrication was procured from Dow Corning Corporation, Midland, MI. A typical fiber yarn contained 500 filaments. The supplier provided information indicates that the diameter of individual filaments in the yarn varies from 8 to 16 μm , and the average filament diameter is $\sim 14 \mu\text{m}$. The as-received fiber yarn had a polyvinyl acetate sizing. The as-received fiber yarns were coated with a dual layer system of $\sim 0.8 \mu\text{m}$ thick BN followed by $\sim 0.2 \mu\text{m}$ thick SiC. The coatings were applied by chemical vapor deposition (CVD) by 3M Corporation, Minneapolis, Minnesota.

2.2. Composite fabrication

The silicon powder required for composite fabrication was obtained from Union Carbide Corporation, Linde Division, Tonawanda, New York. The as-received powder was mixed with a nitride enhancing additive, and the mixture was wet attrition milled in Stoddard solvent (a kerosene-based liquid) for 48h. Attrition milling was performed in a Si_3N_4 vessel using Si_3N_4 grinding media and a

procedure similar to that used by Herbell et al¹³. Attrition milling reduced the particle size of silicon powder from 23 μm to 0.42 μm . The attrition milled silicon powder was dried in an oven maintained at 400⁰C in vacuum for 24h. The dried powder was stored in a glove chamber until further use.

Composites were fabricated by hot pressing a lay-up of silicon coated fiber mats to produce a SiC/Si preform and then nitriding the preform at high temperature in nitrogen. Details of the fabrication are reported by Bhatt and Babuder¹⁴. Here salient features of the composite fabrication will be described. In the first step, a silicon slurry was prepared by ball milling appropriate amounts of attrition milled silicon powder, a polymer binder, a dispersant, and a solvent. The required amount of the slurry was poured into a slurry tank. In the second step, the Hi-Nicalon SiC fiber tow was passed through a series of rollers to spread the tows and then into the tank filled with silicon slurry. The slurry coated fiber tows were wound on a metal drum at a desired spacing to prepare 150 mm wide fiber mat. After drying in air, the fiber mat was removed from the drum, and cut into 150 mm x 150 mm pieces. The cut mat was coated with a 0.5 mm layer of silicon slurry by using a doctor blade apparatus. The composition of the slurry is similar to that used for the fiber coating. When dried, the mats were cut into 12 mm wide strips; some mats were cut parallel and others were cut transverse to the fibers. In the third step, eleven strips all unidirectional, or alternate strips of unidirectional and transverse fiber lay-up were stacked in a stainless steel die and pre-pressed at room temperature. The pre-pressed tapes were hot pressed at 40 MPa at 800⁰C for 15 min to obtain a SiC/Si preform. Subsequently the preform was nitrided in a tube furnace using an appropriate nitridation cycle to convert silicon to silicon nitride matrix. The final dimensions of the specimens after nitriding were 150 mm x 12 mm x 2.5 mm.

2.3. Specimen preparation and testing

The composite panels were surface ground with a diamond particle impregnated metal bonded grinding wheel to remove excess matrix layer present on the surface.

For tensile testing, dog-bone shaped specimens were machined from the composite block by using an ultrasonic SiC slurry impact machine. At each specimen end, two glass fiber-reinforced epoxy tabs of dimension 37 mm x 12 mm x 1 mm were bonded, leaving ~60 mm for the gauge section. A wire wound strain gauge was bonded at the center of the gauge section to monitor the strain during the tensile test. The specimens were tested at room temperature until failure in a servo-controlled tensile testing machine equipped with self aligning grips at a cross-head speed of 1.3 mm/min. Three to five specimens were tested to generate tensile data.

For microstructural examination, some composite specimens were sectioned normal to the fibers, mounted in a metallographic mold, ground successively on 40 μm down to 3 μm diamond particle impregnated metal disks, and polished in a vibratory polisher on a micro cloth using a 0.3 μm diamond powder paste. The mounted specimens were coated with a thin layer of carbon or palladium in a vacuum evaporator to avoid charging during observation in a scanning electron microscope (SEM).

Cyclic fiber push-in tests were performed using a desktop fiber push-out apparatus equipped with capacitance gauges for displacement measurements as previously described¹⁵. The Hi-Nicalon SiC fibers were pushed-in using a 70°-included-angle conical diamond indenter with a 10 μm diameter flat on the bottom. To prevent the sides of the conical indenter from indenting the matrix, the push-in distances were restricted to just a couple of microns.

3. RESULTS AND DISCUSSION

3.1. Physical Properties

The room temperature apparent and skeletal densities were measured to estimate % open porosity in SiC/RBSN composite specimens. The skeletal density was measured by Archimedes method using methylethylketone liquid. The measured data are tabulated in Table I. The data represent an average of five specimens.

Table I. Summary of physical property data for Hi-Nicalon SiC/RBSN composites.

Fiber lay up	Fiber content , vol %	Apparent density, gm/cc	Porosity, vol %
0	24	1.96 \pm 0.02	36 \pm 5
0/90	24	1.94 \pm 0.01	37 \pm 5

3.2. Microstructure

The SEM photographs of the cross-section of 1-D CVD BN/SiC coated Hi-Nicalon SiC/RBSN composites are shown in Fig. 1. A low magnification photograph (Fig. 1(a)) reveals that silicon slurry, hence silicon nitride matrix, is well infiltrated between the filaments in the tows, but between the fiber tows distinct matrix rich regions can be found. Also the matrix is very porous with isolated large pores distributed throughout the cross-section. A higher magnification photograph of the cross-section of the yarn shows that the CVD interface coating on the Hi-Nicalon fibers is non-uniform and irregular (Fig.1(b)). Generally, the thickness of coating on the periphery of the tows was significantly

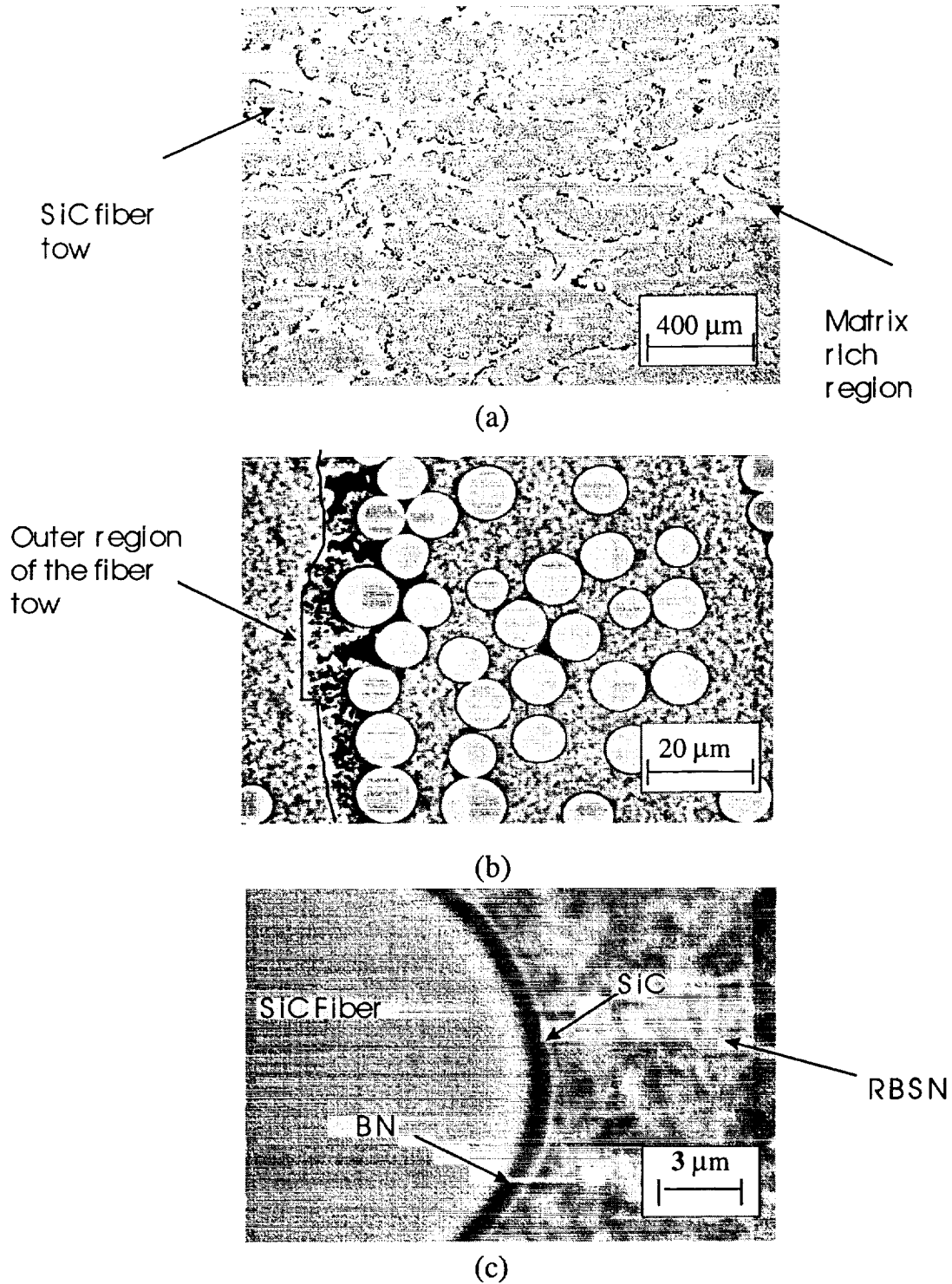


Fig. 1 SEM photographs of a cross-section of 1-D BN/SiC coated Hi-Nicalon SiC/RBSN composites ($V_f \sim 0.24$).

greater than in the interior of the tows. Figure 1 (c) is a photograph of a single SiC filament showing the BN/SiC interface. The darker ring around the fiber is the BN coating and the grayish ring on top of the BN is the SiC coating. The BN coating appears to be uniform, but the SiC coating is generally nodular and rough. TEM analysis of the interface indicates (photographs not shown) that the BN coating is amorphous, and that the SiC coating is crystalline and composed of columnar grains. Figures 1(a) and (b) show that the majority of the RBSN matrix and SiC outer coating interface showed no reaction, but local areas of reaction are present. TEM revealed that the nitride enhancing additive in the RBSN matrix locally reacted with the SiC coating.

3.3. Mechanical behavior of laminated composites

Typical room temperature tensile stress-strain behaviors of $[0]_{10}$ and $[0/90]_s$ BN/SiC coated Hi-Nicalon SiC/RBSN composites (~24 vol%) are shown in Fig. 2. Included in the figure is the tensile stress-strain behavior of the monolithic RBSN matrix fabricated under similar conditions. The stress-strain curve of both 1-D and 2-D reinforced BN/SiC coated Hi-Nicalon SiC/RBSN composites showed two distinct regions: an initial linear region followed by a non-linear region. At ultimate load the composite specimens failed abruptly. In contrast, the stress-strain curve of monolithic RBSN showed only one initial linear region. Also noticed is that the strain capability of both 1-D and 2-D composites is significantly greater than that of the monolithic RBSN. The tensile data are summarized in Table II. The data represent average of 3 to 5 tests.

Figure 3 shows the fracture surface of 1-D BN/SiC coated Hi-Nicalon SiC/RBSN composites. It is obvious from the figure that the composites exhibit a significant amount of fiber pull out, typical of a tough composite. Examination of

the gage section of the fractured specimen indicates a concentration multiple matrix cracks near the main crack which caused fracture.

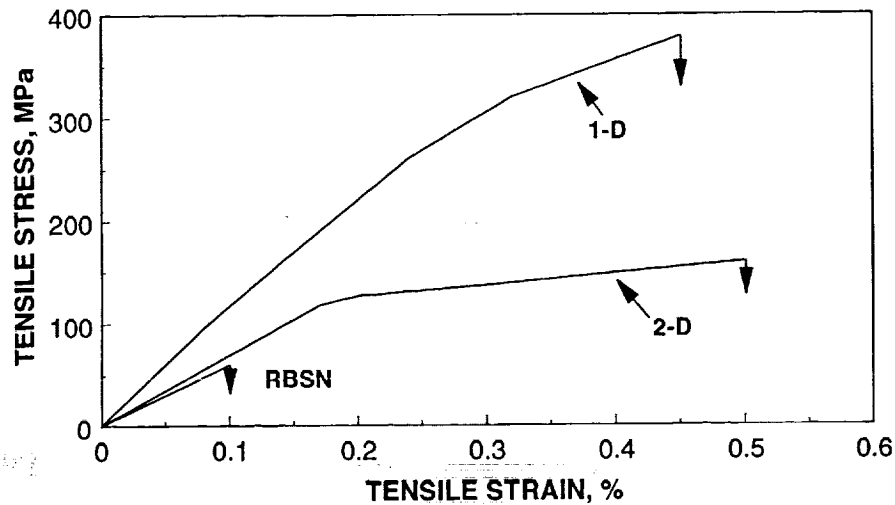


Fig. 2 Typical room temperature tensile-strain curves for 1-D and 2-D BN/SiC coated Hi-Nicalon SiC/RBSN composites ($V_f \sim 0.24$).

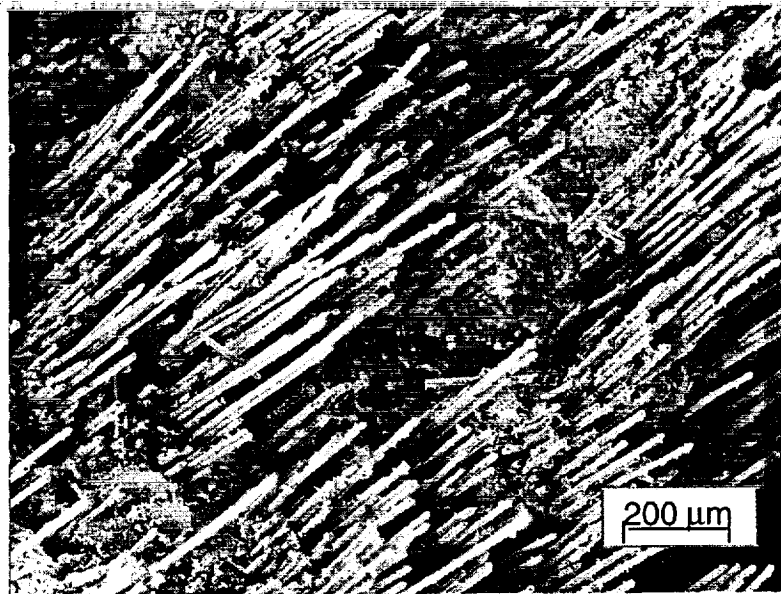


Fig. 3 SEM photograph of the tensile fracture surface of a 1-D BN/SiC coated Hi-Nicalon SiC/RBSN composite ($V_f \sim 0.24$).

Table II. Room temperature tensile property data for Hi-Nicalon SiC/RBSN composites.

Material	Fiber layup	Fiber content, vol %	Proportional limit stress, MPa	Proportional limit strain, %	Elastic modulus, GPa	Ultimate tensile strength, MPa	Ultimate tensile strain, %
RBSN	-	-	60	0.1	60	60	0.1
SiC/RBSN	0	24	298 \pm 13	0.27 \pm 0.01	110 \pm 4	343 \pm 24	0.35 \pm 0.04
SiC/RBSN	0/90	24	84 \pm 16	0.1 \pm 0.01	85 \pm 2	133 \pm 20	0.35 \pm 0.07

3.4. Interfacial shear strength

The room temperature load-displacement curve obtained from the push-in test for 1-D BN/SiC coated Hi-Nicalon SiC/RBSN composites is shown in Fig. 4. The data were analyzed by first subtracting the appropriate load-train compliance correction from the measured displacements. The fiber debond initiation stress was determined and the frictional sliding stresses was estimated. An estimate of frictional sliding stress, τ , was made using the constant τ model of Marshall and Oliver¹⁶ and the following relationship:

$$U = U_0 + F^2 / 8 \Pi^2 r^3 E_f \tau$$

where U is the fiber end displacement, U_0 is the residual fiber end displacement after the previous unloading, F is the applied load, r is the fiber radius, and E_f is the fiber modulus. In addition, a debond initiation stress, σ_d , could be calculated from the debond initiation load, F_d , (load at which fiber end begins to move by the relation $\sigma_d = F_d / \Pi r^2$). The values of measured debond and interfacial shear stresses for this composites are 1.4 GPa and 15.4 MPa respectively.

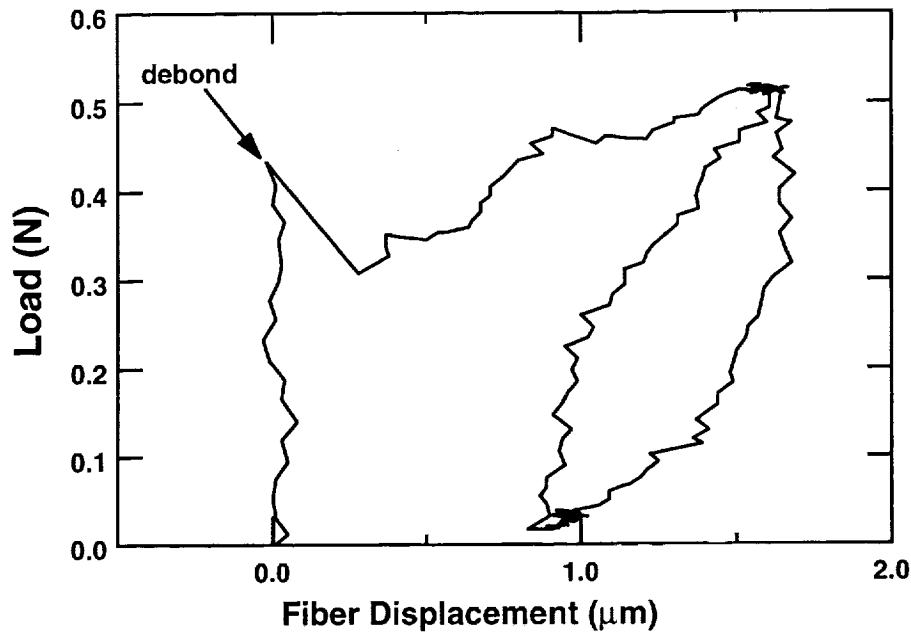


Fig. 4 Typical room temperature fiber push-in test behavior of BN/SiC coated Hi-Nicalon SiC/RBSN composite.

3.5. Matrix cracking strength prediction

A fiber bridging crack model developed by Aveston, Cooper, and Kelly¹⁷ was used to predict the matrix cracking strength in SiC/RBSN composites. For this calculation the following values of $E_f=270$ GPa, $E_m= 60$ GPa, Γ_m (matrix fracture energy) $=36$ J/m², $\alpha_f=3.8 \times 10^{-6}$, $\alpha_m=5.4 \times 10^{-6}$, $\tau = 15$ MPa, $\Delta T=1175$ and $R=7 \times 10^{-6}$ m were used. The variation of matrix cracking strength with fiber fraction was predicted with and without accounting for thermal residual stresses. Results are compared with the measured values in Fig. 5. The plot indicates that the predicted values agree with the measured values.

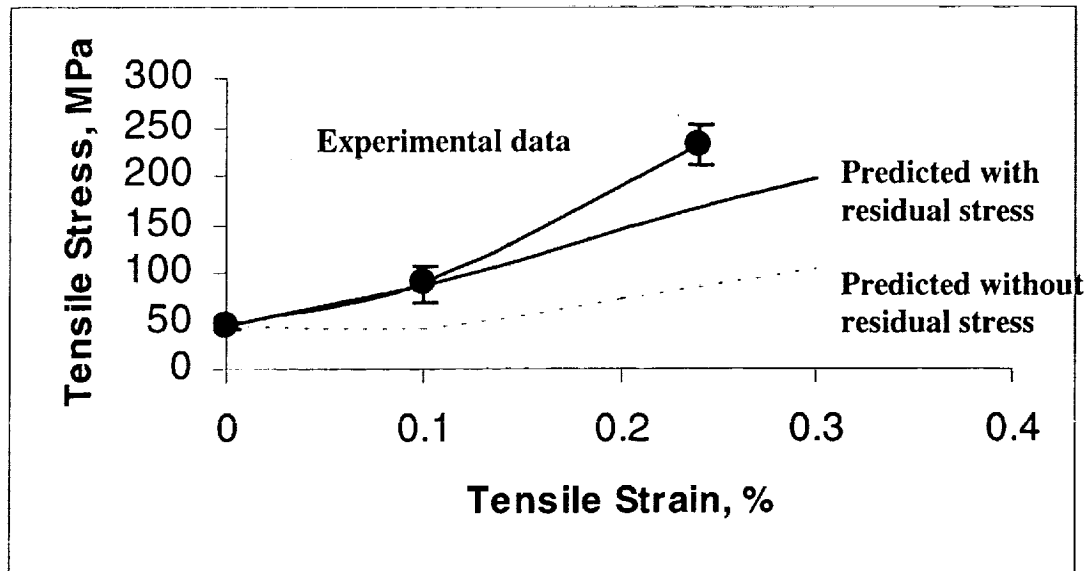


Fig. 5 Experimental data and predictions of first matrix cracking stress by the long fiber-bridging crack model for SiC/RBSN composites.

4. CONCLUSIONS

A strong and tough RBSN can be fabricated by using BN/SiC coated Hi-Nicalon SiC fibers. Further improvements in composite properties are possible by controlling fiber fraction, and processing variables.

ACKNOWLEDGEMENTS

I would like to thank Dr. Jeffrey Eldridge for performing interfacial shear strength measurements and T.A. Leonhardt for preparing the ceramographic specimens

REFERENCES

- 1) F.L. Riley, Nitrogen Ceramics (Noordhoff, Leyden, 1977).
- 2) E.M. LENOE, R.N. KATZ and J.J. BURKE , Ceramics for High Performance Applications, Vol. III (Plenum, New York, London, 1979).
- 3) J.A. MANGELS and G.J. TENNENHOUSE, Bull. Am. Ceram. Soc. **59** [2](1980)1216.
- 4) O.J. GREGORY and M.H. RICHMAN, J. Amer. Ceram. Soc. **67**(1984) 335.
- 5) S. KLEBER and J. H. WEISS, J. Euro. Ceram. Soc. **10**(1992)205.
- 6) R.T. BHATT, U.S. Patent No. 4689188 (1987).
- 7) J.W. LUCEK, G.A. ROSSETTI, Jr., and S.D. HARTLINE, Stability of continuous Si-C(-O) reinforcing elements in reaction-bonded silicon nitride process environments, in: Metal Matrix, Carbon, and Ceramic Matrix Composites 1985, NASA CP-2406, ed. J.D. Buckley, NASA, Washington, D.C.,1985.
- 8) T.L. STARR, D.L. MOHR, W.J. LACKEY, and J.A. HANIGOFFSKY, Ceram. Eng. Sci. Proc., **14** [9-10] 1125-1132 (1993).
- 9) G.H. WOBLEWSKA and G. ZIEGLER, Ceramic Trans. **58**, 131-136 (1995).
- 10) M. TAKEDA, Y. IMAI, H. ICHIKAWA, T. ISIKAWA, N. KASAI, T. SEGUCHI, and K. OKAMURA, Ceram. Eng. Sci. Proc., **13** (7-8), 209-217 (1992).
- 11) J.B. HURST, D. GORICAN, and H.M. YUN, Ceramic Trans. **58**, 131-136 (1995).
- 12) R.T. BHATT and D.R. HULL, Effects of fiber coatings on tensile properties of

Hi-Nicalon SiC/RBSN tow composites, NASA TM-113170, NASA, Washington, D.C. 1997.

13) T.P. HERBELL, T.K. GLASGOW and N.W. ORTH, Bull. Amer. Ceram. Soc. **63** [9](1984) 1176.

14) R.T. BHATT and R. BABUDER, Processing and properties of Hi-Nicalon SiC/RBSN composites, NASA TM (in press).

15) J.I. ELDRIDGE, Desktop fiber push-out apparatus, NASA TM-105341, NASA, Washington, D.C., 1991.

16) D.B. MARSHALL and W.C. OLIVER, Mater. Sci. Eng. A, 126, 95-103 (1990).

17) J. AVESTON, G. COOPER, and A. KELLY, Single and multiple fracture, in: The Properties of Fiber Composites (Conference Proceedings, National Physical Laboratory, Guildford) IPC Science and Technology Press Ltd., 1971.

Please make following corrections to the authors proof.

- (1) Page 1, right column, last sentence: a period after (BN)/SiC.
- (2) Page 3, second column heading of the Table I should read Fiber content (vol %).
- (3) Page 4, third column heading of the Table II should read Fiber content (vol%).
- (4) Page 5, left column: delete the forth line.
- (5) Suggested keywords list: A. Tape casting/hot pressing. B. Composites. C. Mechanical properties. D. SiC/Si₃N₄. E. Structural applications

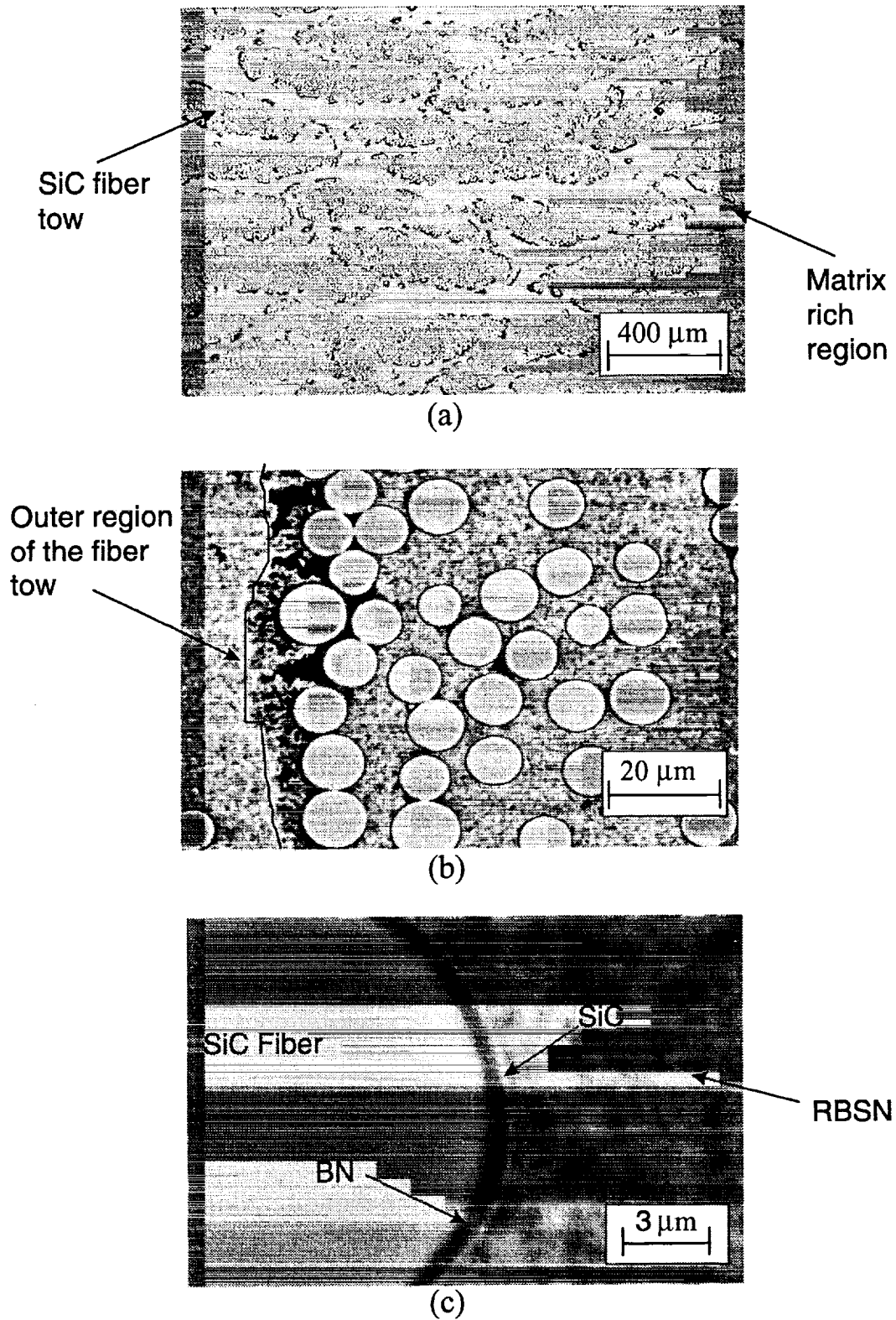


Figure 1. SEM photographs of a cross-section of 1-D BN/SiC coated Hi-Nicalon SiC/RBSN composites ($V_f \sim 0.24$).

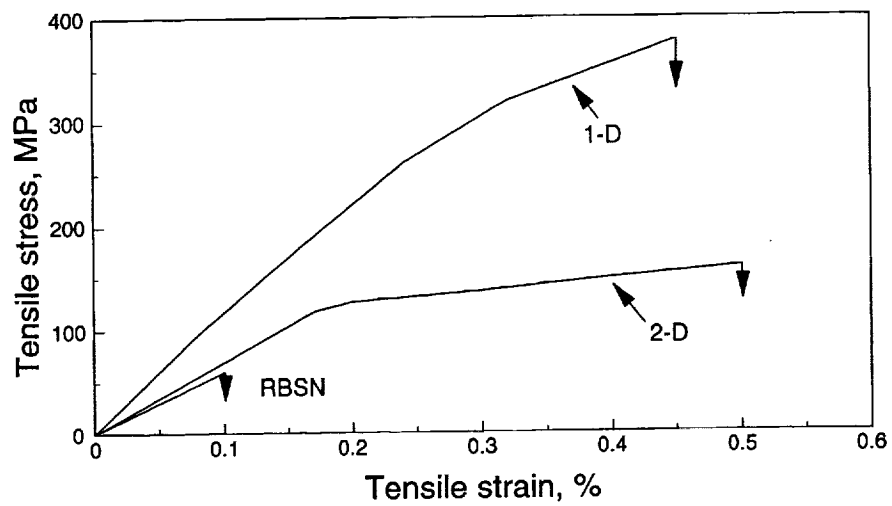


Figure 2. Typical room temperature tensile-strain curves for 1-D and 2-D BN/SiC coated Hi-Nicalon SiC/RBSN composites ($V_f \sim 0.24$).

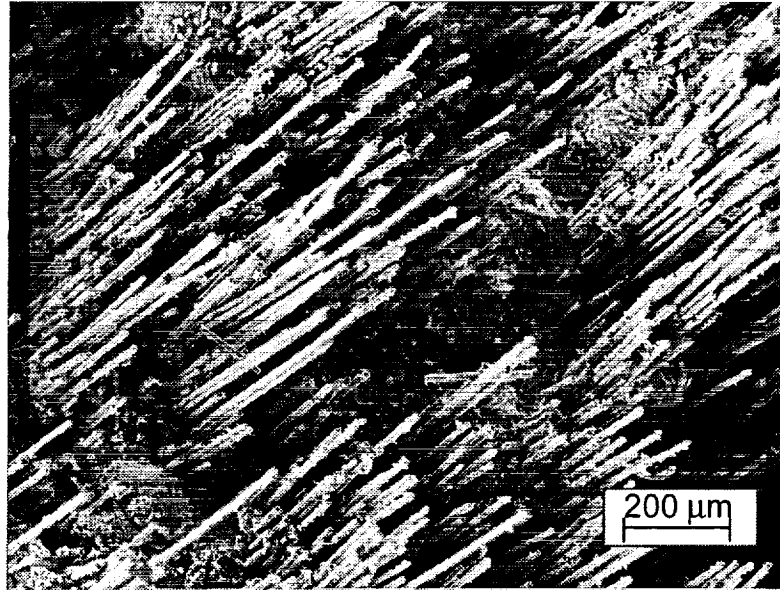


Figure 3. SEM photographs of the tensile fracture surface of a 1-D BN/SiC coated Hi-Nicalon SiC/RBSN composites ($V_f \sim 0.24$).

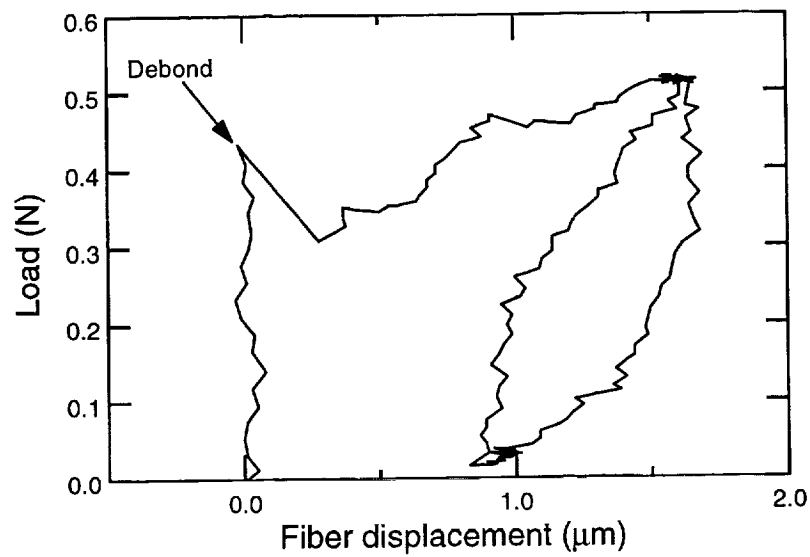


Figure 4. Typical room temperature fiber push-in test behavior of BN/SiC coated Hi-Nicalon SiC/RBSN composite.

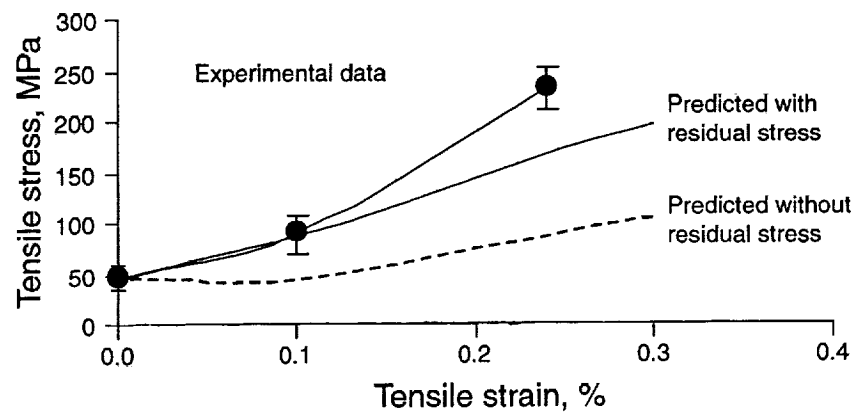


Figure 5. Experimental data and predictions of first matrix cracking stress by the long fiber-bridging crack model for SiC/RBSN composites.